Regional, Directional, and Age-Dependent Properties of the Brain Undergoing Large Deformation

Michael T. Prange
e-mail: mprange@exponent.com

Susan S. Margulies[1]
e-mail: margulies@seas.upenn.edu

Department of Bioengineering,
University of Pennsylvania,
3320 Smith Walk,
Philadelphia, PA 19104-6392

The large strain mechanical properties of adult porcine gray and white matter brain tissues were measured in shear and confirmed in compression. Consistent with local neuroarchitecture, gray matter showed the least amount of anisotropy, and corpus callosum exhibited the greatest degree of anisotropy. Mean regional properties were significantly distinct, demonstrating that brain tissue is inhomogeneous. Fresh adult human brain tissue properties were slightly stiffer than adult porcine properties but considerably less stiff than the human autopsy data in the literature. Mixed porcine gray/white matter samples were obtained from animals at "infant" and "toddler" stages of neurological development, and shear properties compared to those in the adult. Only the infant properties were significantly different (stiffer) from the adult. [DOI: 10.1115/1.1449907]

Introduction

In the United States, traumatic brain injury (TBI) is a leading cause of death and disability. Approximately 1.5 million Americans experience TBI per year and incidences requiring hospitalization or death number 300,000–550,000 annually [1,2]. In children, TBI is the most common cause of death and TBI resulting in hospitalization or death occur in at least 150,000 children per year, at a rate of over 200 per 100,000 children [3]. Diffuse white matter damage is associated with a large fraction of those patients with poor neurologic outcome in adult and pediatric survivors of brain injury, ranging from subtle behavioral changes to significant neurologic deficits. Biomechanical analyses of diffuse axonal injury (DAI) suggest a link between brain material response (strain) and white matter injury [4–9]. Understanding the biomechanics of diffuse brain injuries in adults and children requires the development of a precise relationship between the macroscopic head motions and the mechanical response of the brain.

In order to gain insight into the mechanisms of traumatic brain injury, computational modeling is often used to estimate intracranial deformations during traumatic loading. The accuracy in predicting the circumstances that cause DAI using these models is dependent on the biofidelity of the material properties. It is essential that material properties are defined separately for different regions, directions, ages and account for the potential nonlinear viscoelastic behavior at finite strains because the inhomogeneous, anisotropic, and age dependent tissue properties can influence the resulting deformations within the brain. Studies have shown large strains occurring during rapid head rotations [5,10] and injury thresholds above 20 percent strain [11,12]. Therefore it is also critical for brain material properties to be examined and characterized at large deformation.

Material properties of brain tissue have been measured during compression, shear, and oscillatory loading [13–24] and the reported properties vary from study to study, within and across modes of testing, by as much as an order of magnitude. This range is probably related to the anisotropic and inhomogeneous nature of brain tissue and the broad range of test conditions.

White matter consists of a fiber arrangement that is highly oriented, while gray matter consists of cell bodies and supporting vascular network that likely do not impose such directional preference. Magnetic resonance diffusion tensor images of the brain neuroarchitecture confirm that some regions of white matter can be modeled as transversely isotropic, while gray matter is an isotropic structure [25]. Despite this evidence, though, few investigators have examined directional properties of brain tissue. To our knowledge, only Shuck and Advani included the anisotropy and inhomogeneity of brain in their study design [23]. However, Shuck and Advani's important and encouraging data were obtained at very small strains of 1.3 percent, considerably smaller than those associated with traumatic head injury.

Previously, brain tissue has been idealized as an isotropic material at large deformations. As a first step to evaluate the validity of this approximation, this paper presents data defining the regional and directional properties of adult brain tissue at strains up to 50 percent. We hypothesize that gray matter has an isotropic tissue structure. Previously the brainstem was demonstrated to be a transversely isotropic material that can be accurately represented by a fiber-reinforced composite where the uniaxially oriented viscoelastic fibers (neural tracts) are three times stiffer than the surrounding viscoelastic matrix (extracellular components and oligodendrocytes) [26]. Because oriented neural tracts also exist within the cerebral white matter, we hypothesize white matter would also be a transversely isotropic material, and that within the white matter, the ratio of moduli depends on the extent of fiber orientation. Two regions of cerebral white matter, the corpus callosum and corona radiata, were examined to test this hypothesis. The corpus callosum is a highly aligned, uniaxially oriented region of the brain consisting of neural tracts running between the left and right hemispheres. We expect that this region will resemble previous findings in the brainstem. In contrast, the corona radiata is also composed of neural tracts, but the tissue is not uniaxially oriented; the fibers appear in a 'fan' pattern along a major axis. we expect that the corona radiata has a smaller difference in the moduli between direction than the corpus callosum consistent with a less aligned organization.

Traditionally, a biomechanical analysis of head injury in the infant and young child assumes that they respond as miniature adults, with identical tissue properties and injury thresholds [27–31]. Using dimensional analysis, critical inertial loading conditions associated with DAI were scaled from the adult to the infant as a function of brain mass [32]. These studies concluded that the

[1]To whom all correspondence should be addressed.

Contributed by the Bioengineering Division for publication in the JOURNAL OF BIOMECHANICAL ENGINEERING. Manuscript received by the Bioengineering Division Oct. 17, 2000; revised manuscript received Oct. 25, 2001. Associate Editor: R. Vanderby, Jr.

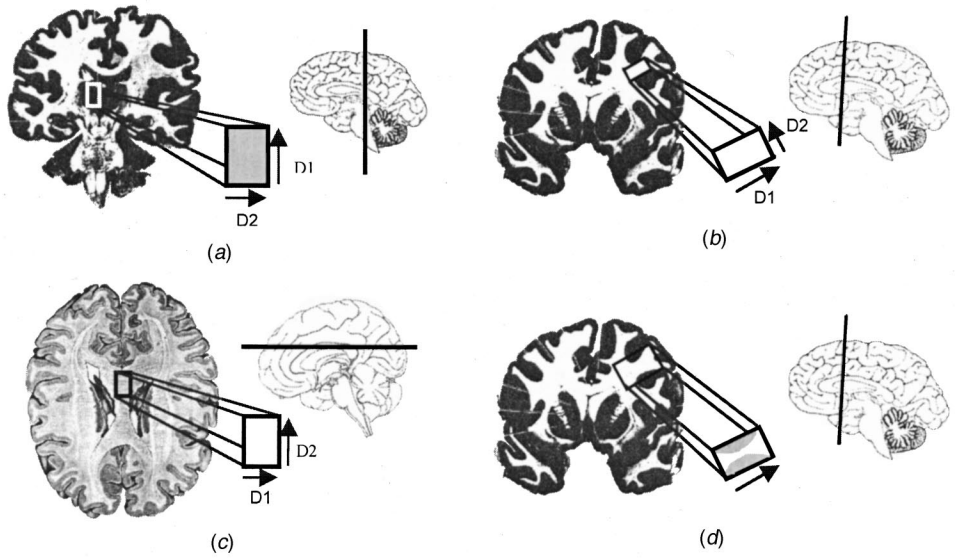

Fig. 1 Anatomic locations and test directions (D1= direction 1, D2=direction 2) of (*a*) adult gray matter sample and (*b*) adult corona radiata sample shown in coronal section (left) and sagittal section (right). Anatomic location of (*c*) adult corpus callosum sample shown in transverse section (left) and sagittal section (right). Anatomic locations and test direction of (*d*) five-day and four-week old mixed white/gray matter samples shown in coronal section (left) and sagittal section (right).

lower brain mass of the young child allows the pediatric brain to sustain higher rotational accelerations than its adult counterpart before the onset of injury. However, alterations in tissue composition and mechanical properties can influence the resulting deformations and, in turn, injury patterns within the brain. Recently, Melvin and Hymel recognized the important role of material properties in defining age-specific injury mechanisms and thresholds, and emphasized the current lack of age-related material property data within the literature [33,34]. Only Thibault and Margulies have investigated the age-dependency of brain material properties, and although their analysis found a significant difference between infant and adult porcine tissue, the study tested samples only at small strains ($\leqslant$2.5 percent) [24]. In addition to adult tissue properties, this paper presents data describing the properties of infant and toddler brain tissue at large strains, up to 50 percent.

In summary, the focus of this paper is on a critical gap in the existing literature: identifying the anisotropy, inhomogeneity, and age-dependent nature of brain tissue at large strains. We hypothesize the white matter is anisotropic due to its cellular architecture, while the gray matter would possess much less directional dependence in its material properties. Furthermore, we hypothesize that brain tissue material properties are inhomogeneous and age-dependent.

Methods

Sample Procurement and Preparation. To test brain tissue for inhomogeneity and anisotropy, rectangular tissue samples (10 $\times$5$\times$1 mm) were excised from porcine sections of white matter (corona radiata and corpus callosum) and gray matter (thalamus) maintaining consistent orientation from animal to animal. The cause of death of the adult animals was rapid exsanguination while the pediatric animals were sacrificed using a lethal dose of KCl or pentobarbital. All samples were transported in 4°C mock cerebral spinal fluid (CSF) solution and tested within 5 hours postmortem [35]. Specimen dimensions (length, width, thickness) were measured in triplicate with a digital caliper and averaged.

In the gray matter, Direction 1 (D1) was defined as the superior/inferior direction, and Direction 2 (D2) was defined as the transverse direction in the coronal plane (Fig. 1(*a*)). In corona radiata samples, D1 was defined as aligned with the neural tracts in the coronal plane, and D2 was defined as orthogonal to the tracts in the coronal plane (Fig. 1(*b*)). In the corpus callosum samples, D1 was defined as aligned with the neural tracts in the transverse plane and D2 was defined as orthogonal to the tracks in the transverse plane (Fig. 1(*c*)). Each sample was tested along only one direction. Eighteen corona radiata white matter samples (12 D1, 6 D2), 12 corpus callosum samples (6 D1, 6 D2) and 18 gray matter samples (12 D1, 6 D2) were tested from a total of 32 brains.

To test brain tissue properties for age-dependency, tissue samples were excised from five-day old (n=6) and four-week old (n=5) piglets which have the composition and neurologic development equivalent to a human newborn ($<$1 month old) and toddler (approximately one–three years), respectively [36]. The rectangular samples were taken from the same location as the corona radiata samples of the adult and tested along D1 (Fig. 1(*d*)). Because of the smaller brain size, these tissue samples consisted of a mixture of approximately equal amounts of white (corona radiata) and gray matter. These data were compared with average white and gray matter properties of the adult porcine data.

Fresh human remnant temporal cortex samples (gray matter, N=5), obtained from the operating suite after temporal lobectomy procedures, were tested within three hours after excision. Data were compared with porcine tissue data. All protocols were approved by the University of Pennsylvania IACUC and IRB.

Shear Testing Protocol. Using a custom designed, humidified, parallel-plate shear testing device [37], displacement and force were measured during rapid stress relaxation tests in simple shear. The tissue was held in place between the glass plates without adhesive and with negligible pre-compression. The bottom plate was displaced with a ramp time of 60 msec and hold time of 60 sec in the following order of approximate strain (ε_{12}) magnitudes: 2.5 percent, 5 percent, 10 percent, 20 percent, 30 percent, 40 percent, 50 percent, and retested at 5 percent to confirm reproducibility. Each specimen was tested at strain rates ranging between 0.42 and 8.33 s^{-1}. Steady state was verified at 60 sec for all tissue types and directions with less than a 0.5 percent change in stress over the last five seconds and the specimen was allowed to relax for 60 sec before the next test was performed.

Data were obtained (1 kHz sampling rate) at each strain level after two preconditioning runs at that strain level and stored on computer. For each strain level, force and displacement data at five isochrones (100 msec, 300 msec, 800 msec, 1800 msec, and 60 sec after peak) from each specimen were evaluated to determine the properties for the specified tissue type and direction.

Validation in Unconfined Compression. Following the shear testing, unconfined compression experiments were conducted to test the validity of the constitutive model in a different testing mode. Gray matter samples ($10\times5\times2.5$ mm, $n=4$) were compressed using a stress relaxation protocol at 5 percent, 30 percent, and 50 percent strain (ε_{22}). The tissue was placed in a parallel plate indentor and the top plate controlled by a stepper motor (Model 26449-05, Haydon Switch and Instrument, Inc., Waterbury, CT). The displacement of the top plate was measured with an LVDT (Model 0241, Trans-Tek, Inc, Ellington, CT) and the resulting compressive force was measured with an axial force transducer (Model 31, Sensotec, Columbus, OH). The plates were lubricated (Braycote 804 Grease, Castol, Irvine, CA) to ensure a pure slip boundary that was confirmed photographically. The displacement ramp rate was approximately 1.5 mm/sec (strain rate of 0.6 sec^{-1}), followed by a 60 sec hold. Data were obtained at each strain level after two preconditioning runs were performed. The measured long-term nominal stress values ($t=60$ sec) were compared to the predictions of the long-term nominal stress generated for unconfined compression using the constitutive model and the parameters determined from the shear tests.

Interfacial Conditions for Testing Device. Studies were designed to confirm that the shear testing protocol provided a no-slip boundary condition at the two glass plates and was nondestructive to the tissue. The no-slip boundary condition was examined by marking the tissue, displacing the bottom plate 1mm ($\varepsilon_{12}=50$ percent), and measuring the displacement of the tissue at the top plate from photographs. The tissue was marked with cresyl violet and a 25 mm grid secured on the top glass plate. The locations of five points on the tissue were digitized at the top tissue surface relative to the grid and compared to the digitizing error.

Tissue Integrity Assessment. To demonstrate that the testing protocol did not damage the tissue, a mixed gray/white matter sample near the corona radiata was subjected to 50 percent shear strain and compared to an unstrained sample obtained from the same excised brain specimen. Both samples were fixed and microtome sections were stained with a Nissl stain to examine cellular integrity. The cell bodies' size, shape, distribution, organization, and stain intensity were compared.

An additional assessment of the tissue integrity was conducted comparing the final test at 5 percent shear strain after the entire multitest protocol was completed. The long-term moduli (G_∞) of the initial and final 5 percent tests of ten random samples were compared with a paired Student's t test. If the samples were not damaged during the test, these two test conditions were expected to yield similar results.

Analysis

A strain energy-based constitutive model was developed to describe the behavior of white and gray matter in orthogonal simple shear tests. Isotropy and homogeneity were assumed for each sample tested, and a comparison of properties obtained in different directions was employed to evaluate anisotropy. The nonlinear material properties were modeled with a first-order Ogden hyperelastic model modified to include energy dissipation. In this approach, the analysis started with a formulation for an elastic material based on a first-order Ogden hyperelastic material with a strain energy density function W [38]:

$$W=\frac{2\mu}{\alpha^2}(\lambda_1^{\alpha}+\lambda_2^{\alpha}+\lambda_3^{\alpha}-3) \tag{1}$$

where α and μ are properties of the material, and λs are the principal stretch ratios. The parameter α incorporates the strain-magnitude sensitive nonlinear characteristics, and μ corresponds to the shear modulus of the tissue. In simple shear ($\lambda_3=1$), the maximum principal stretch ratio λ is related to the engineering shear strain γ ($2\varepsilon_{12}$) [38]:

$$\lambda=\frac{\gamma}{2}+\left(1+\frac{\gamma^2}{4}\right)^{1/2}. \tag{2}$$

Assuming incompressibility ($\lambda_1\cdot\lambda_2\cdot\lambda_3=1$), the elastic component of the shear stress (T_{12}) measured on top face of the tissue sample is related to the applied shear:

$$T_{12}=\frac{2\mu}{\alpha}\frac{(\lambda^{\alpha}-\lambda^{-\alpha})}{(\lambda+\lambda^{-1})}. \tag{3}$$

To incorporate time-dependent behavior, the shear modulus in the above expression (μ) was replaced with a modulus that changes with time, $\mu(t)$. This formulation assumes that α is independent of time and $\mu(t)$ is independent of strain.

To determine the parameter α in our constitutive relationship independently of μ, isochrone data was examined from our stress relaxation tests. At a fixed stress isochrone ($t=t_i$), the measured stress response across the seven different strain magnitudes tested

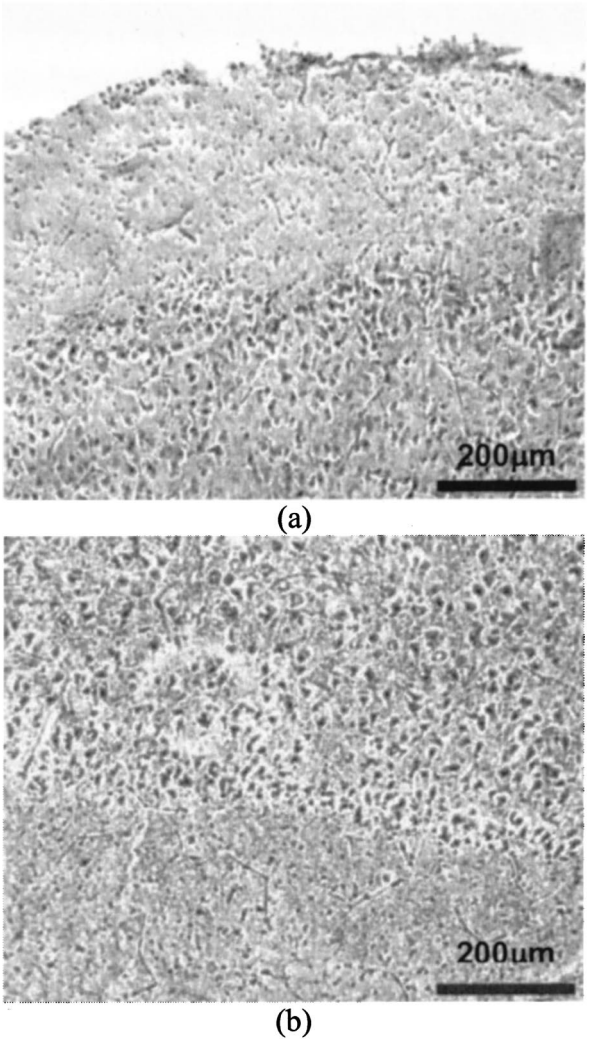

Fig. 2 Representative histology slides of control tissue (*a*) and strained (50 percent) tissue (*b*).

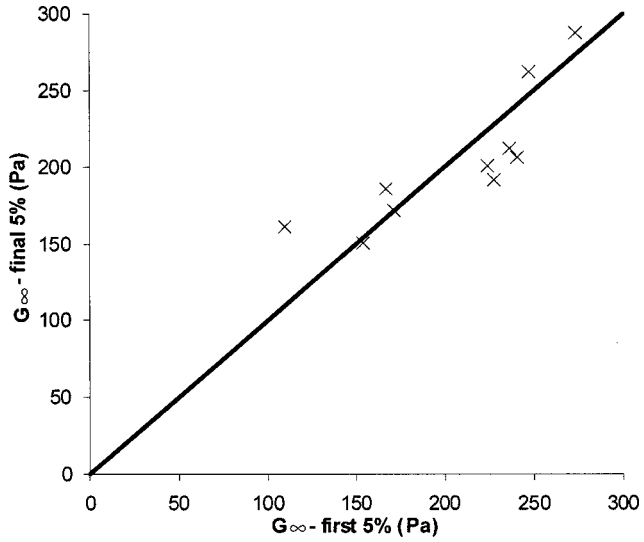

Fig. 3 Long-term shear moduli of first and final 5 percent shear strain tests (line has slope=1).

was normalized to the stress at a specific shear level ($\gamma = \gamma_0$). This yielded the following expression for normalized shear at time t_i that was independent of μ:

$$T_{12,\text{norm}}(\lambda, t_i) = \frac{(\lambda^{\alpha} - \lambda^{-\alpha})(\lambda_0 + \lambda_0^{-1})}{(\lambda_0^{\alpha} - \lambda_0^{-\alpha})(\lambda + \lambda^{-1})} \tag{4}$$

where λ_0 is the principal stretch at the shear γ_0. Using the definitions above, T_{12}, γ, and λ values were calculated at each isochrone from the force and displacement data recorded from all ramp-and-hold stress relaxation experiments and normalized the values to $\gamma_0 = 0.50$ ($\varepsilon_{12} = 25$ percent). The stress at 25 percent strain was determined by interpolating between the stress measured at the 20 percent and 30 percent shear strain tests. To determine α for the first-order Ogden model, all isochrone and strain data for a particular tissue and test direction was combined and fit to Eq. (4) using a least-squares nonlinear regression (IGOR Pro 3.1.4, Wavemetrics, Lake Oswego, OR). To confirm that the overall α value was time-independent, Eq. (4) at each isochrone was evaluated as well.

Once α was determined, the measured relaxation response was re-analyzed at each isochrone to determine the relaxation modulus $\mu(t)$. Using the overall α determined for that tissue type and direction, Eq. (3) was rearranged to solve for μ at each isochrone to calculate the shear relaxation modulus $\mu(t_i)$ directly at each of these times t_i.

$$\mu_i(t_i) = \frac{\alpha T_{12}(\lambda + \lambda^{-1})}{2(\lambda^{\alpha} - \lambda^{-\alpha})} \tag{5}$$

To determine μ at a specific isochrone, all strain data of all samples for a particular tissue region and test direction at that time point was combined and fit to Eq. (5) using least-squares linear regression through the origin. To confirm that $\mu(t)$ was independent of λ, the data at individual strain levels used to fit to Eq. (5), were evaluated. The values of $\mu(t)$ at each time point were compared statistically using Student's t analyses for comparing two slopes to determine if there were any significant differences between the corona radiata, corpus callosum, human temporal cortex or gray matter properties and if there were any significant differences between direction within a tissue type. The data at each isochrone were then combined into a single second-order Prony series for a particular region and test direction:

$$\mu(t) = \mu_0 \left(1 - \sum_{i=1}^{2} C_i (1 - e^{-t/\tau_i}) \right). \tag{6}$$

Results

Interfacial Testing Condition. The assumption of a no-slip boundary condition for the shear testing mode was confirmed with the analysis of displacement of the tissue at the top plate during the largest tissue strain ($\varepsilon_{12} = 50$ percent). The five points digitized had an average displacement of 0.009 mm with a digitizing error of 0.008 mm. The tissue displacement was statistically indistinguishable from the digitizing error and was less than 1 percent of the displacement of the bottom plate.

The pure slip condition between the plates and tissue in the unconfined compression tests was evaluated photographically. Given a bulk modulus of approximately 2 MPa (300,000 psi) [39], the brain tissue was assumed to be incompressible. The change in surface area of the tissue samples, evaluated at 50 percent compression, differed less than 1 percent from that predicted for an incompressible material, confirming the pure slip boundary at the plates is a valid assumption for this testing mode.

Tissue Integrity Assessment. The Nissl staining revealed no difference between the unstrained tissue and tissue strained with the 50 percent shear strain protocol (Fig. 2). The cell bodies had similar size, shape, distribution, organization, and stain intensity, indicating no tissue discernable damage as a result of the testing protocol. Tissue damage for the shear testing mode was also verified by examining the mechanical properties before and after a sample was subjected to 50 percent shear strain. Figure 3 shows an identity plot of G_∞ of the first and final 5 percent shear strain test for each sample. The plot shows no consistent pattern between the first and final shear modulus. Paired–t analysis of the long-term moduli (G_∞) of the first and final 5 percent (ε_{12}) shear strain were not significantly different ($p = 0.83$, $n = 10$), demonstrating the testing protocol did not alter the tissue.

Shear Material Properties. No consistent influence of time was found on the Eq. (4) relationship nor of strain on the Eq. (5) relationship, confirming that the response of gray matter and white matter samples tested in a single direction could be represented using this modified hyperelastic material model. The parameters for each tissue type and direction are shown in Tables 1 and 2.

The coefficient of determination (R^2) was $\geqslant 87$ percent for each fit to Eq. (4), supporting the Ogden model as an appropriate material model to represent the nonlinearity of brain tissue (Fig. 4). The α value was varied for each tissue region and direction to determine the sensitivity of the curve fit to the α value. The R^2 value changed less than 1 percent when α was varied by an order of magnitude (0.001–0.8). Therefore, given the relatively narrow

Table 1 Ogden coefficients α and $\mu(t)$ (Eq. 6)) for porcine adult regions, directions

Age/Species	Adult Porcine								
Region	Gray Matter (thalamus)			Corona Radiata			Corpus Callosum		
Direction	D1	D2	avg	D1	D2	avg	D1	D2	avg
# samples	12	6	18	12	6	18	6	6	12
α	0.0273	0.0600	0.0382	0.0741	0.0360	0.0614	0.0497	0.0759	0.0628
μ_0 (Pa)	271.5	256.1	263.6	292.6	211.4	254.2	131.4	232.2	182.2
C_1	0.302	0.296	0.300	0.288	0.265	0.279	0.297	0.264	0.276
τ_1 (sec)	2.71	2.49	2.60	2.86	2.42	2.72	2.590	3.03	2.85
C_2	0.451	0.478	0.464	0.497	0.516	0.505	0.474	0.462	0.466
τ_2 (sec)	0.186	0.165	0.175	0.167	0.167	0.166	0.151	0.162	0.158

Table 2 Ogden coefficients α and $\mu(t)$ (Eq. (6)) for human adult, porcine adult, porcine 5-day and 4-week old tissue

Species	Human	Porcine	
Region	Gray matter	Mixed Gray/White Matter	
Age	Adult	5 day	4 week
# samples	6	6	5
α	0.0323	0.0100	0.0326
μ_0 (Pa)	295.7	526.9	216.5
C_1	0.335	0.332	0.316
τ_1 (sec)	2.40	2.96	3.00
C_2	0.461	0.389	0.428
τ_2 (sec)	0.146	0.181	0.190

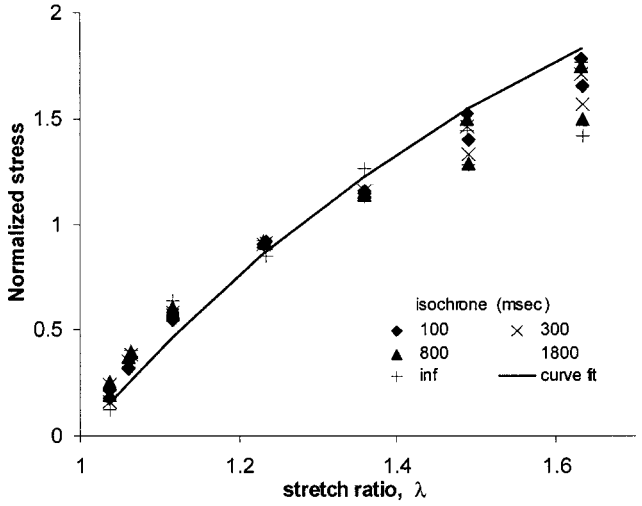

Fig. 4 Typical nonlinear regression to determine the constant α. Data shown for 1 sample.

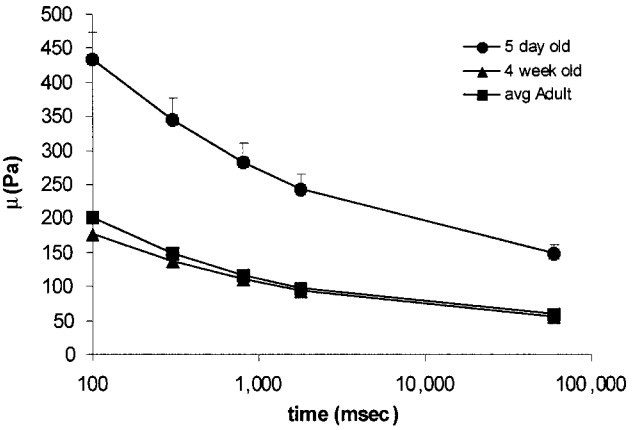

Fig. 6 Age-dependent properties. Time-dependent Ogden component μ for five-day old piglet, four-week old piglet, and average adult porcine white and gray matter properties (error bars indicate 95 percent confidence interval)

range of α values reported in Tables 1 and 2 (0.0100–0.0759), that values of α were determined not vary significantly across either tissue type or direction.

To compare human and porcine properties, a mean porcine gray matter $\mu(t)$ was computed from the average D1 and D2 properties at each isochrone. At each isochrone, $\mu(t)$ was significantly different between human gray matter ($n=5$) and porcine gray matter ($n=18$) ($p<0.05$, Fig. 5). The human samples were an average of 29 percent (37.7 Pa) stiffer than the porcine samples.

After averaging the D1 and D2 properties to obtain mean values for the adult corona radiata and gray matter, a combined adult white/gray matter $\mu(t)$ was calculated at each isochrone by averaging the mean values of these two regions, in order to compare mixed porcine properties across different ages. At each isochrone, $\mu(t)$ of the five-day old piglet ($n=6$) was significantly higher than the combined white/gray matter adult properties ($n=36$) ($p<0.001$), and higher than the four-week old piglet ($n=5$) ($p<0.001$, Fig. 6). Specifically, the five-day old piglet samples were, on average, two times stiffer than the adult specimens. In contrast, the four-week $\mu(t)$ values were not significantly different from the adult properties at any isochrone.

To evaluate regional inhomogeneity, a mean $\mu(t)$ was calculated from the average D1 and D2 within each region at each isochrone (Fig. 7). The corpus callosum region was significantly

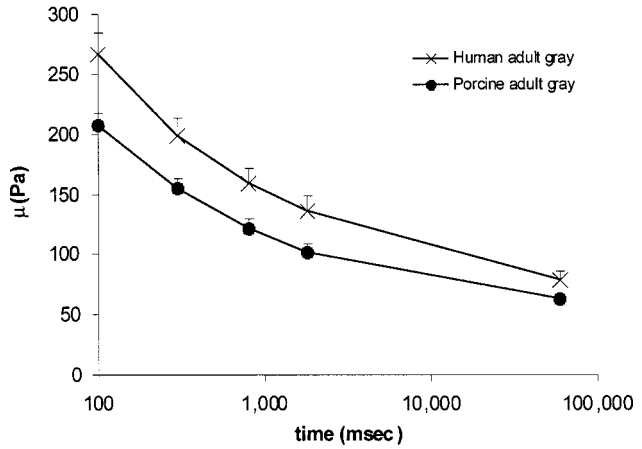

Fig. 5 Time-dependent Ogden parameter μ for human and porcine gray matter (error bars indicate 95 percent confidence interval)

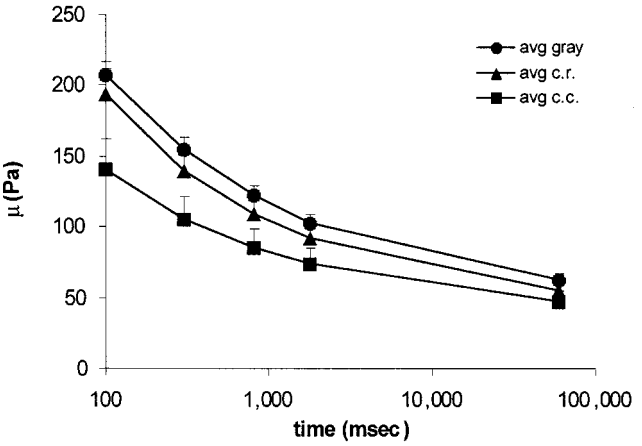

Fig. 7 Regional properties. Time-dependent Ogden component μ for corona radiata (c.r.), corpus callosum (c.c.), and gray matter (error bars indicate 95 percent confidence interval).

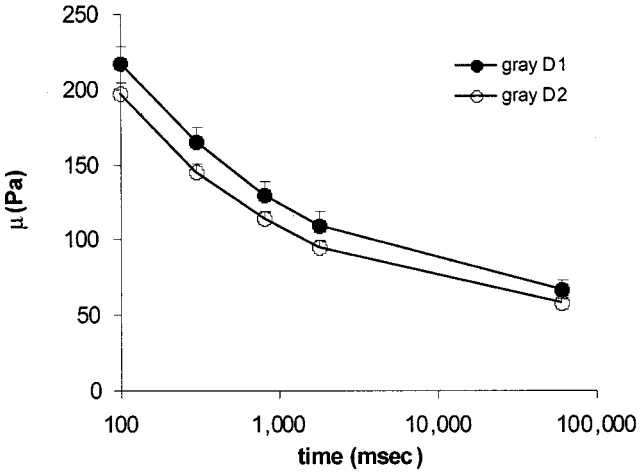

Fig. 8 Directional properties. Time-dependent Ogden component μ for gray matter (error bars indicate 95 percent confidence interval).

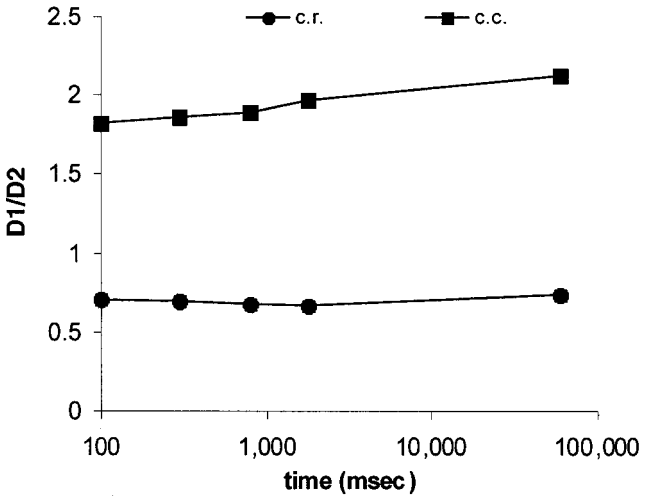

Fig. 10 Directional properties. Direction ratio (D1/D2) or gray matter, corona radiata (c.r.) and corpus callosum (c.c.).

different from the gray matter at every time point ($p<0.001$) while the corona radiata and gray matter regions were statistically indistinguishable from each other ($p>0.09$). Corpus callosum properties were statistically different from the corona radiata region at the first two isochrones, but were not significantly different at the 800 msec, 1800 msec, and 60 sec isochrones (Fig. 7). Gray matter had the largest average μ while corpus callosum had the lowest average μ at every time point.

To evaluate intraregional anisotropy, comparisons were made between D1 and D2 results obtained from each region. Gray matter showed no difference between the two orthogonal directions ($p>0.07$, Fig. 8). However, directions 1 and 2 for each white matter type were significantly different ($p<0.02$), but only corpus callosum had D2 properties greater that D1 (Fig. 9). The ratio (D2/D1) of μ was evaluated at each time point and averaged to yield approximately 0.70 and 1.93 for corona radiata and corpus callosum, respectively (Fig. 10).

To evaluate directional properties across regions, comparisons were made between the corona radiata and corpus callosum results obtained from the same direction. Corona radiata was significantly ($p<0.001$) stiffer than corpus callosum for D1 (parallel to fiber direction) at all time points. Direction 2 properties were statistically indistinguishable between the two white matter regions at all isochrones ($p>0.1$, Fig. 9).

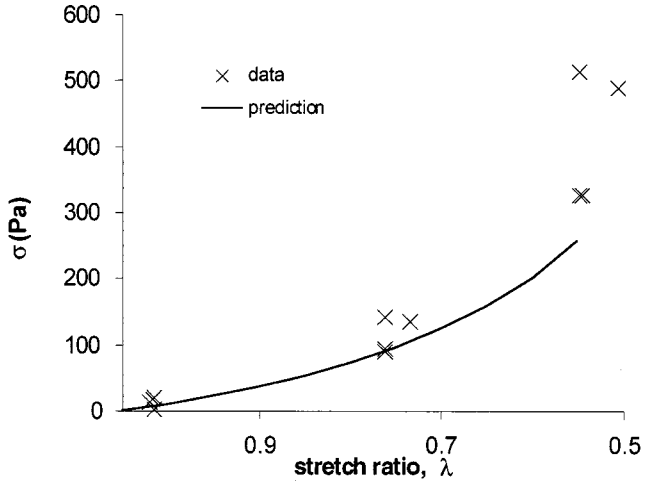

Fig. 11 Long-term stress of unconfined compression experiments compared to prediction of Ogden material model

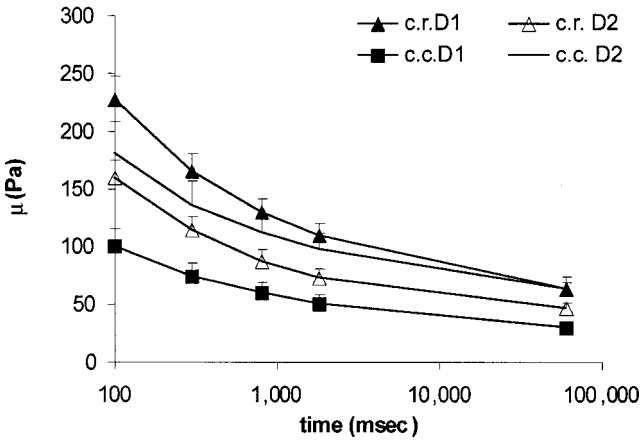

Fig. 9 Directional properties. Time-dependent Ogden component μ for white matter regions corona radiata (c.r.) and corpus callosum (c.c.) (error bars indicate 95 percent confidence interval).

Taken together, these findings from the porcine shear tests support our hypotheses that white matter and gray matter have distinct properties, and that white matter behavior is more anisotropic than gray matter. These findings also support the hypotheses that different degrees of anisotropy exist within the white matter, a finding that we propose correlates with the neurostructural organization in these regions.

Validation in Unconfined Compression. Results for unconfined compression of porcine gray matter samples showed a typical relaxation response to the ramp and hold compression. The measured long-term stress values from the gray matter compression experiments conducted are shown in Fig. 11. Using the average material parameters describing the shear properties of gray matter, these measured compression results were compared to the predictions of the modified Ogden hyperelastic model. The results show excellent agreement, with a R^2 value of 84 percent for the prediction, thus validating this material model in a second independent test mode.

Discussion

In the current research, finite element modeling is the primary tool used to predict the mechanisms of TBI. However, the material properties used in these computational models are crucial for accurately predicting the circumstances that cause TBI. This extensive determination of the mechanical properties of brain tissue at large strains, including the effects of region, direction, age and species, represents a major step forward in our understanding of the response of the brain during traumatic events. As such, it is important to compare these findings with the limited data in the literature obtained using other models, testing modes, strain magnitudes, and sample conditions.

Brain material properties in the past have been measured in vitro during compression, shear and oscillatory loading [13–20,22–24]. The reported properties vary from study to study, within and across modes of testing, by as much as an order of magnitude. The broad range of testing methods (large range of strain rates and magnitudes, different species, locations, specimen preparations, and testing modes) along with the nonlinearity of brain tissue makes comparisons difficult. A continuum of strains within a single sample were tested to overcome the difficulty of comparing small strain and finite strain properties across different samples or tests. The results of experiments at higher strain rates show that this modified hyperelastic model for brain tissue is valid for a large range of strain rates (up to 8.33 s^{-1}). In addition, the nonlinearity of the samples could be modeled for both testing protocols employed.

To overcome difficulty with comparing material representations of brain tissue developed for different testing modes, unconfined compression tests were employed to validate the material model in a different mode of deformation. The compression results were in excellent agreement with the predicted response using the material parameters found from the simple shear tests (Fig. 11), showing the modified Ogden hyperelastic material model can be used to accurately represent brain tissue material properties. Studies have shown that fluid flow in tissue can cause a change in mechanical properties and this could account for this small difference between the compression and shear tests [40]. Our long-term stress relaxation behavior to an applied step displacement in unconfined compression tests is approximately five to ten times more compliant than material properties reported by Mendis et al. and Miller et al. [18–21]. The stiffer properties previously reported may be attributable testing conditions and tissue handling, such as the lack of preconditioning of the specimen, or postmortem storage conditions.

The properties determined in this paper for adult brain tissue correlate most closely with previous large deformation simple shear studies performed by Donnelly and Medige [15]. The nonlinear viscoelastic model determined by Donnelly and Medige for a constant rate displacement in simple shear was compared to our data. The nonlinear nature of this model fit our data well at 5 percent and 50 percent but the properties in the literature were approximately 4.25 times stiffer at both strains than those obtained in the present study. These material properties reported previously may be stiffer because they were determined from experiments conducted at least 12 hours postmortem, as well as using different strain rates and specimen locations than those used in the present study.

Due to the difficulty in obtaining human brain samples, porcine tissue is often used as a substitute for brain material testing [14,19,24,26]. However, other laboratories have tested human tissue obtained at autopsy to avoid potential phylogenic differences in the properties [15,16,23,41]. The advantage of using porcine brain tissue is that it is easily procured and can be tested shortly after death, therefore reducing the effects of the tissue degradation on the mechanical properties. The relative difference between porcine tissue and a limited series of fresh human material were examined to determine if any significant species differences existed in the mechanical behavior. To our knowledge, the human surgical sample data in this paper were obtained at much earlier time points after excision than previous studies, and are the only fresh, nonautopsy human data available. These human temporal lobe gray matter samples ($n=5$) were compared to the porcine gray matter samples and were found to be stiffer (29 percent) at every time point (Fig. 5). The human specimens were obtained from temporal lobectomies performed on epilepsy patients. Therefore, the difference between the human and porcine tissue properties may be attributable to the abnormal human samples. Of note, though, is that these fresh human tissue properties are considerably less stiff than the human autopsy data in the literature, placing it far closer to fresh porcine data tested at large strain than human autopsy data.

The porcine mechanical properties of brain tissue for infant piglets and adult pigs were found to be significantly different from each other (Fig. 6). Specifically, the pediatric Ogden parameter μ was approximately two times greater than the adult at every time point. In contrast, Thibault and Margulies found significantly stiffer properties in adult tissue compared with pediatric brain tissue when measured at 1.25 percent shear strain, over a frequency range (20–200 Hz), and no significant difference between adult and pediatric tissue at 2.5 percent shear strain. [24]. However, performing these measurements at large deformation reveals that brain tissue is nonlinear, and that adult tissue is stiffer than pediatric tissue at very small strains, but not at large strains. Considering only the 20 Hz, 2.5 percent strain test condition, which is similar to the present study in strain magnitude and rate, Thibault and Margulies found the shear modulus for pediatric tissue was higher than adult tissue, but did not reach the level of statistical significance ($p=0.21$). Limiting our analysis of the present data set to only our combined adult and five-day old tissue data at 2.5 percent strain, fit to a standard linear model as in the previous report, our small strain moduli for the adult and 5-day old samples were indistinguishable from the corresponding tissue properties reported by Thibault and Margulies ($p=0.97$ and 0.07 respectively) also showing a higher shear modulus for pediatric tissue than the adult ($p<0.001$). It is important to reemphasize that the present study reveals that this trend of stiffer pediatric properties extends to large deformations.

Previous studies have investigated regional inhomogeneity in the brain, but they were limited to small oscillatory strains, and the results were reported using linear viscoelastic material models. Specifically, properties of the cerebrum [24] and brainstem [13,42] were studied in shear, and the corona radiata and thalamic gray matter in torsion [23]. To compare the current data to these previous reports, only our small strain data (2.5 percent, combining directions 1 and 2) were fit to a standard linear model. All three regions were significantly less stiff than the brainstem [42]. In contrast to our large strain findings, when only small strain data were considered there were no significant differences in the complex moduli between our three regions studied. Similarly, Shuck and Advani reported no significant differences in complex moduli between coronal radiata and gray matter at very low levels of strain (1.3 percent) and strain rates (<0.26 s^{-1}) [23].

These distinctions between large and small strain behavior underscore the importance of characterizing the material behavior over the full range of distortions experienced during traumatic loads applied to the head. At large strains, when D1 and D2 data were combined, regional shear tests revealed significant differences between corpus callosum, and the other two regions at the faster time points (100 and 300 msec). Across time (t_i), gray matter and corona radiata were the stiffest regions and corpus callosum the most compliant, with gray matter and corona radiata approximately 30 percent stiffer than corpus callosum. Because mechanical property differences between regions are only apparent at the shorter time points, inhomogeneity may be important only for rapid events, rather than slower, crushing head injuries. This regional inhomogeneity results in stress/strain concentrations

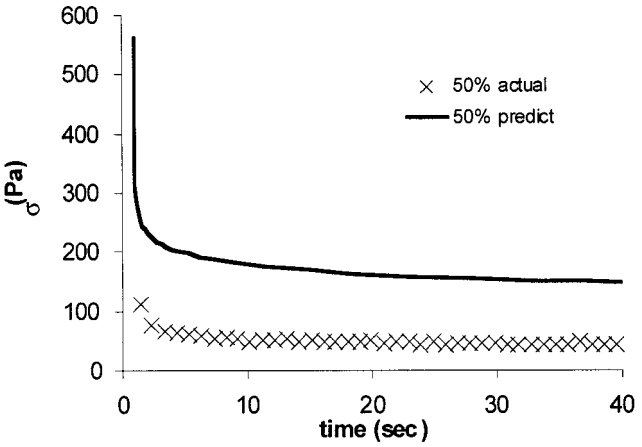

Fig. 12 Prediction of linear fifth-order Maxwell model

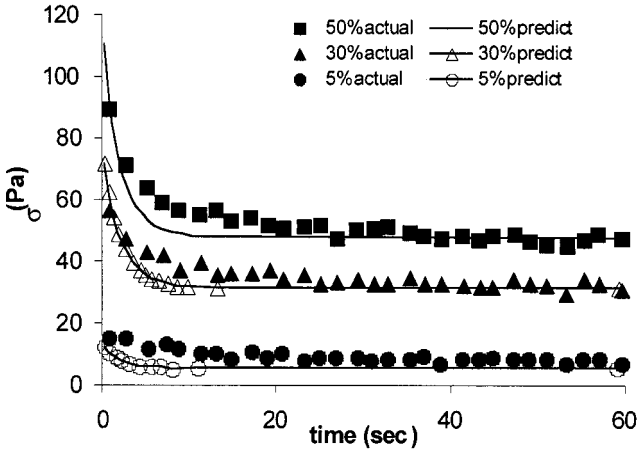

Fig. 13 Prediction of Ogden hyperelastic model modified to include dissipation

that may play important roles in the regional tissue injury patterns reported in traumatic head injuries such as diffuse axonal injury and gliding contusions.

In addition to regional inhomogeneity, our large strain shear tests demonstrate anisotropy within the white matter regions but not within the gray matter. Examination of the gray matter showed no difference in directional properties, supporting our hypothesis that gray matter is an isotropic region at large deformations. In contrast, corpus callosum properties were 1.93 times stiffer in D2 than D1. This finding is consistent with a uniaxial, fiber-reinforced model that was proposed previously for brainstem, with stiff viscoelastic fibers surrounded by a viscoelastic matrix [26]. In contrast, corona radiata samples revealed D1 properties greater than D2.

Although the corpus callosum region studied has a highly oriented, uniaxial structure, the corona radiata region also includes fibers that extend perpendicular to the major axis. A high proportion of these off-axis fibers would result in an increase in D1 modulus and decrease in D2 modulus. In fact, D1 properties of the corona radiata were indeed stiffer than those of the corpus callosum and the D2 properties of the corona radiata are less stiff than corpus callosum. Thus, development and examination of a multiaxial composite model would be more suitable for the corona radiata. The next step is to develop an anisotropic testing protocol and material model to accurately describe the white matter tissue response to more complex deformations.

The nonlinear material model developed in this report appears to be a more representative material model for brain tissue across a broad range of strains compared to a linear viscoelastic representation. To demonstrate this point, our small strain data (5 percent) was fit to a 5th-order linear Maxwell model and LS-DYNA (Livermore Software Technology Corp., Livermore, CA) was used to predict the 50 percent strain response in simple shear. As seen in Fig. 12, the Maxwell model overestimated the shear stress at 50 percent shear strain. A similar finite element simulation was performed using ABAQUS Explicit 5.7 (HKS Inc., Pawtucket, RI) and the Ogden hyperelastic model modified to include dissipation. This model accurately predicts the shear stress at the top face of the tissue at all strains ranging from 5 percent to 50 percent (Fig. 13). The applicability of the Ogden material representation across a range of strains believed to encompass injury conditions [11,12,29], as well as its availability for use in commercial finite element packages, points to a new opportunity for modeling the response of the human head to impact using this improved material model. The dramatic difference in behavior between the linear and nonlinear representations at finite strains suggests that future modeling results for human head finite element models employing the modified Ogden formulation may show similar and important differences from those using linear or elastic descriptions.

Taken together, good agreement was found between our data obtained at small strains and those published previously in the literature for fresh brain tissue [14,24,42]. However, brain tissue is nonlinear, and its large strain behavior reveals some notable differences. In summary, brain tissue properties show significant inhomogeneity at large strains (up to 50 percent) between corpus callosum and gray matter, and even between two white matter regions—corona radiata and corpus callosum. Specifically, the average gray matter properties are 1.3 times stiffer than the most compliant region, the corpus callosum. Second, gray matter was shown to be isotropic; however, significant anisotropy exists in both white matter regions tested, with the degree of anisotropy correlated with local neuroarchitecture. Third, brain tissue properties are age-dependent, with infant tissue being approximately twice as stiff as adult tissue. Fourth, a modified Ogden hyperelastic formulation is an effective material model for brain tissue undergoing large deformations in either shear or compression. Fifth, fresh porcine and human brain tissues are approximately four to ten times less stiff than previous reports in the literature for autopsy specimens. These large strain, regional, directional, and age-specific data should enhance the biofidelity of computational models and provide important information regarding the mechanisms of traumatic brain injury.

Acknowledgments

Funds were provided by the Center for Injury Prevention and Control at the Centers for Disease Control (R49/CCR-312712). The authors are grateful to Dr. David Meaney for his helpful discussions about material models and for performing the finite element simulations of simple shear, Drs. A. C. Duhaime and G. H. Baltuch for their cooperation in providing surgical specimens, Gail Alderfer and Bart Hoffman at Hatfield Quality Meats of Hatfield, PA for providing the adult porcine tissue, Dr. W. M. Armstead for providing the infant porcine samples, and John Noon for the design of the tissue indentor system.

References

[1] Sosin, D. M., Sniezek, J. E., and Waxweiler, R. J., 1995, "Trends in Death Associated with Traumatic Brain Injury, 1979 Through 1992. Success and Failure," J. Am. Med. Assoc., **273**, pp. 1778–1780.
[2] Thurman, D. J., Alverson, C., Dunn, K. A., Guerrero, J., and Sniezek, J. E., 1999, "Traumatic Brain Injury in the United States: A Public Health Perspective," J. Head Trauma Rahabil., **14**, pp. 602–615.
[3] CDC, 1990, "Childhood Injuries in the United States," Am. J. Dis. Child, **144**, pp. 627–646.
[4] Lee, M., Melvin, J., and Ueno, K., 1987, "Finite Element Analysis of Traumatic Subdural Hematoma," *Proc of 31st Stapp Car Crash Conference.*
[5] Margulies, S., Thibault, L., and Gennarelli, T., 1990, "Physical Model Simulations of Brain Injury in the Primate," J. Biomech., **23**, pp. 823–836.

[6] Meaney, D., Smith, D., Ross, D., and Gennarelli, T., 1995, ''Biomechanical Analysis of Experimental Diffuse Axonal Injury,'' J. Neurotrauma, **12**, pp. 311–322.
[7] Mendis, K., 1992, *Finite Element Modeling of the Brain to Establish Diffuse Axonal Injury Criteria*, Ohio State University.
[8] Miller, R., Margulies, S., Leoni, M., Nonaka, M., Chen, X., Smith, D., and Meaney, D., 1998, ''Finite Element Modeling Approaches for Predicting Injury in an Experimental Model of Severe Diffuse Axonal Injury,'' *Proc. of 42nd Stapp Car Crash Conference*.
[9] Zhou, C., Khalil, T., and King, A., 1995, ''A New Model Comparing Impact Responses of the Homogeneous and Inhomogeneous Human Brain,'' *Proc. of 39th Stapp Car Crash Conference*.
[10] Misra, J., and Chakravarty, S., 1984, ''A Study on Rotational Brain Injury,'' J. Biomech., **17**, pp. 459–466.
[11] Bain, A., and Meaney, D., 1999, ''Thresholds for Mechanical Injury to the In Vivo White Matter,'' *Proc. of 43rd Stapp Car Crash Conference*.
[12] Shrieber, D., Bain, A., and Meaney, D., 1997, ''In Vivo Threshold for Mechanical Injury to the Blood-Brain Barrier,'' *Proc. of 41st Stapp Car Crash Conference*.
[13] Arbogast, K., and Margulies, S., 1998, ''Material Characterization of the Brainstem from Oscillatory Shear Tests,'' J. Biomech. **31**, No. 9, pp. 801–807.
[14] Brands, D., Bovendeerd, P., Peters, G., Wisman, J., Paas, M., and Bree, J.v., 1999, ''Comparison of the Dynamic Behaviour of Brain Tissue and Two Model Materials,'' *Proc. of 43rd Stapp Car Crash Conference.*
[15] Donnelly, B., and Medige, J., 1997, ''Shear Properties of Human Brain Tissue,'' ASME J. Biomech. Eng., **119**, pp. 423–432.
[16] Fallenstein, G., and Hulce, V., 1969, ''Dynamic Mechanical Properties of Human Brain Tissue,'' J. Biomech., **2**, pp. 217–226.
[17] Galford, J., and McElhaney, J., 1970, ''A Viscoelastic Study of Scalp, Brain, and Dura,'' J. Biomech., **3**, pp. 211–221.
[18] Mendis, K., Stalnaker, R., and Advani, S., 1995, ''A Constitutive Relationship for Large Deformation Finite Element Modeling of Brain Tissue,'' ASME J. Biomech. Eng., **117**, pp. 279–285.
[19] Miller, K., and Chinzei, K., 1997, ''Constitutive Modeling of Brain Tissue: Experiment and Theory,'' J. Biomech., **30**, pp. 1115–1121.
[20] Miller, K., 1999, ''Constitutive Model of Brain Tissue Suitable for Finite Element Analysis of Surgical Procedures,'' J. Biomech., **32**, pp. 531–537.
[21] Miller, K., Chinzei, K., Orssengo, G., and Bednarz, P., 2000, ''Mechanical Properties of Brain Tissue In-Vivo: Experiment and Computer Simulation,'' J. Biomech., **33**, pp. 1369–1376.
[22] Prange, M., Kiralyfalvi, G., and Margulies, S., 1999, ''Pediatric Rotational Inertial Brain Injury: The Relative Influence of Brain Size and Mechanical Properties,'' *Proc. of 43rd Stapp Car Crash Conference.*
[23] Shuck, L., and Advani, S., 1972, ''Rheological Response of Human Brain Tissue in Shear,'' J. Basic Eng., **94**, pp. 905–911.
[24] Thibault, K., and Margulies, S., 1998, ''Age-Dependent Material Properties of the Porcine Cerebrum: Effect on Pediatric Inertial Head Injury Criteria,'' J. Biomech., **31**, pp. 1119–1126.
[25] Pieropaoli, C, and Basser, P., 1996, ''Toward a Quantitative Assessment of Diffusion Anisotropy,'' Magn. Reson. Med., **36**, pp. 893–906.
[26] Arbogast, K., and Margulies, S., 1999, ''A Fiber-Reinforced Composite Model of the Viscoelastic Behavior of the Brainstem in Shear,'' J. Biomech., **32**, pp. 865–870.
[27] Dejeammes, M., Tarriere, C., Thomas, C., and Kallieris, D., 1984, ''Exploration of Biomechanical Data Towards a Better Evaluation of Tolerance for Children Involved in Automotive Accidents,'' SAE Trans., **No. 840530**, pp. 427–441.
[28] Duhaime, A., Gennarelli, T., Thibault, L., Bruce, D., Margulies, S., and Wiser, R., 1987, ''The Shaken Baby Syndrome: A Clinical, Pathological, and Biomechanical Study,'' J. Neurosurg., **66**, pp. 409–415.
[29] Margulies, S., and Thibault, L., 1992, ''A Proposed Tolerance Criterion for Diffuse Axonal Injury in Man,'' J. Biomech., **25**, pp. 917–923.
[30] Mohan, D., Bowman, B., Snyder, R., and Foust, D., 1979, ''A Biomechanical Analysis of Head Impact Injuries to Children,'' ASME J. Biomech. Eng., **101**, pp. 250–260.
[31] Sturtz, G., 1980, ''Biomechanical Data of Children,'' SAE Trans., **No. 801313**, pp. 513–559.
[32] Ommaya, A., Yarnell, P., Hirsch, A., and Harris, E., 1967, ''Scaling of Experimental Data on Cerebral Concussion in Sub-human Primates to Concussion Threshold for Man,'' *Proc. of 11th Stapp Car Crash Conference.*
[33] Hymel, K., Bandak, F., Partington, M., and Winston, K., 1998, ''Abusive Head Trauma? A Biomechanics-Based Approach,'' Child Maltreatment, **3**, pp. 116–128.
[34] Melvin, J., 1995, ''Injury Assessment Reference Values for the Crabi 6-Month Infant Dummy in a Rear-Facing Infant Restraint with Airbag Deployment,'' SAE Trans., **No. 950872**, pp. 1–12.
[35] Mock cerebrospinal fluid (CSF): KCl 0.220 g, MgCl 0.132 g, $CaCl_2$ 0.221 g, NaCl 7.71 g, urea 0.402 g, dextrose 0.665 g, $NaHCO_3$ 2.066 g, distilled water 1000 ml.
[36] Duhaime, A. C., Margulies, S. S., Durham, S. R., O'Rourke, M. M., Golden, J. A., Marwaha, S., and Raghupathi, R., 2000, ''Maturation-dependent response of the piglet brain to scaled cortical impact,'' J. Neurosurg., **93**, pp. 455–462.
[37] Arbogast, K., Thibault, K., Pinheiro, B., Winey, K., and Margulies, S., 1997, ''A High Frequency Shear Device for Testing Soft Biological Tissues,'' J. Biomech., **30**, pp. 757–759.
[38] Ogden, R., 1984, *Nonlinear Elastic Deformations*, Ellis Harwood Ltd., Chichester, England (reprinted by Dover Publications, Inc., Mineola, New York, 1997).
[39] McElhaney, J., Roberts, V., and Hilyard, J., 1976, *Handbook of Human Tolerance*, Japan Automobile Research Institute, Tokyo.
[40] Mow, V. C., Holmes, M. H., and Lai, W. M., 1984, ''Fluid Transport and Mechanical Properties of Articular Cartilage: A Review,'' J. Biomech., **17**, pp. 377–394.
[41] Estes, M., and McElhaney, J., 1970, ''Response of Brain Tissue to Compressive Loading,'' *Proc. of Fourth ASME Biomechanics Conference*.
[42] Arbogast, K., and Margulies, S., 1997, ''Regional Differences in Mechanical Properties of the Central Nervous System,'' *Proc. of 41st Stapp Car Crash Conference*.